Extended Abstracts of the 2012 International Conference on Solid State Devices and Materials, Kyoto, 2012, pp388-389

PS-11-15L

Novel IrO_x nanodots based capacitive pH sensor

P. Kumar[1], A. Prakash[1], W. Banerjee[1], and S. Maikap*
[1]Thin Film Nano Tech. Lab., Department of Electronic Engineering, Chang Gung University, Kwei-Shan, Tao-Yuan, 333, Taiwan
*Tel: 886-3-2118800 ext. 5785 Fax: 886-3-2118507 E-mail: sidhu@mail.cgu.edu.tw

1. Introduction

In recent years, EIS structure has drawn major attention among the various semiconductor based biosensors such as ISFET, EIS, and LAPS etc. because of its simplicity in layout, label free detection, easy and cost effective fabrication. Nanoparticles have shown their potential as major diagnostic tool in biological detection because of their unique size dependent electronic, optical and spectroscopic properties due to their small size and comparative high surface area [1]. Very few studies have been reported towards nanoparticles modified EIS structures. Various nanostructure metal oxides have been used as transducers for biosensor such as ZnO, ZrO_x, TiO_x etc. which have shown their functional biocompatibility, non-toxic and high catalytic efficiency [2]. Nanostructured iridium oxide (IrO_x) has attracted more attention due to its promising properties such as chemical stability and good adsorption properties for the biomolecules immobilization. IrO_x shows good response to charge variation at interface because it maintains high charge transfer ratio [3]. As iridium oxide nanostructure are compatible with intracellular material, IrO_x based sensors has been developed to detect biochemical such as enzymes, antibodies and hybridized DNA. Presence of IrO_x nanostructure facilitates the control of the morphology and wettability of the surface which ultimately results in the enhanced sensitivity, single molecule detection and significant reduction in analyte concentration. Recently, W. D. Huang et al. [4] reported the IrO_x film as an electrochemical pH sensor [4], however IrO_x nanodots (NDs) modified EIS structure as capacitive pH sensor has not been reported yet. This novel IrO_x–NDs based pH sensor shows a promising sensing performance with a near-Nernstian response in sensitivity repeatedly and reversibly in between 46.4-52.4 mV/pH in the pH range between 2 and 12 at 25°C.

2. Experiment

p-Type Si (100) substrate was cleaned by the RCA process to remove native oxide from the surface. After RCA cleaning, a 40 nm-thick SiO_2 layer was grown as an insulating layer by dry oxidation process at 1000°C. Then, the IrO_x nano-layer with a nominal thickness of ~ 1nm was deposited by reactive rf sputtering. The Ir target was used for the deposition of IrO_x layer. To fabricate the EIS chip, first a 300 nm-thick Al film was deposited on the back side of the samples after removing the back side oxide using buffer oxide etching solution (BOE). The sensing membrane area was defined by standard photolithography process using a negative photoresist-SU8. Then, EIS devices were attached on a printed circuit board having copper lines. Then, an epoxy layer was used to encapsulate the EIS structure and the copper line. A schematic view of the major fabrication steps of IrO_x-NDs modified EIS sensor are shown in Fig. 1. The capacitance-voltage (C–V) measurements were performed with Agilent 4284A by substrate bias through an Ag/AgCl reference electrode.

3. Results and discussion

Figs.1 (a) – (d) show the schematic view of fabrication process as well as the physical characterization of the iridium oxide modified EIS sensor. After IrO_x NDs deposition on SiO_2 surface, their distribution was confirmed by STEM and HRTEM images, as shown in Fig. 1(c). High density ($1.18x10^{13}/cm^2$) of self-assembled IrO_x-NDs is clearly observed from the large view of STEM images. Size of IrO_x NDs is in range of 1.5nm to 2.5nm as calculated from the high-resolution TEM image. A schematic view of EIS sensor chip is shown in Fig. 1(d). Charge trapping properties of IrO_x–NDs in an $IrO_x/Al_2O_3/IrO_x$-NDs/Al_2O_3/n-Si structure are observed, which prove the available Ir-O dangling bonds on the surface of IrO_x-NDs (Fig. 2).

Presence of IrO_x-NDs on SiO_2 layer is confirmed with EDX analysis, as shown in Figs. 3 & 4. As IrO_x –NDs deposited on SiO_2 surface using RF sputtering in presence of equal ratio of argon and oxygen, two oxidation states of IrO_x was expected on SiO_2 surface that was confirmed with the XPS analysis (Figs. 5 & 6). pH sensing behavior of bare EIS sensor and IrO_x-NDs modified EIS sensor was characterized by typical C-V measurements at different pH buffer solutions, as shown in Figs. 7 & 8. Sensitivity of EIS sensor is calculated from the linear depletion region of the C-V curve. A respective shift in flat band is observed according to the different concentration of hydrogen ions in buffer solutions. Sensitivity of EIS sensor is calculated using the following equation:-

$$\text{Sensitivity} = \frac{\Delta V_{fb}}{\Delta pH} \quad [1]$$

IrO_x-NDs modified EIS sensor showing comparatively high sensitivity for hydrogen ions as compared to bare SiO_2 EIS sensor. This behavior shows the high charge transfer properties of IrO_x. Mechanism of the surface reaction of IrO_x-NDs in different pH environment can be explained by the reactions [5] as follows:-

$$Ir_2O_3 + 6H^+ + 6e^- \leftrightarrow 2Ir + 3H_2O \quad [2]$$

$$IrO_2 + 4H^+ + 4e^- \leftrightarrow Ir + 2H_2O \quad [3]$$

$$2IrO_2 + 2H^+ + 2e^- \leftrightarrow Ir_2O_3 + H_2O \quad [4]$$

At high acidic conditions, more reduction takes place at IrO_x surface that leads to band bending ultimately work function of IrO_x and result in high flat band voltage compared to high pH buffer solution. IrO_x modified EIS sensor showing high average sensitivity of 48.4mV/pH with very good linearity of 99.94% while bare SiO_2 showing sensitivity of 33-35mV/pH with linearity of 98.35% (Fig. 9). Standard error measurement of three IrO_x EIS sensor shows less deviation and high repeatability of EIS sensor device (Fig. 10). Fig. 11 shows concap response of IrO_x-NDs modified EIS sensor that proves the stability and confirms the repeatability of IrO_x NDs modified EIS sensor.

4. Conclusion

A novel IrO_x-NDs based capacitive pH sensor chip has been fabricated and characterized for the first time. IrO_x-NDs modified EIS sensors showing comparatively high sensitivity of 48.8mV/pH with linearity of 99.94% (with a near-Nernstian response in sensitivity) than that of the bare SiO_2 sensor showing sensitivity of ~ 35mV/pH with the linearity of 98.35%. Easy as-deposited and self-assembled IrO_x-NDs based Ph sensor fabrication, good repeatability and high stability paves a way in future biosensor applications.

Acknowledgment

This work was supported by National Science Council (NSC), Taiwan, under the contract no. NSC-101-2221-E-182-061 and also submitted project on biosensor.

References

[1] A.N. Shipway, et al. Chem. Phys. Chem., vol. 1, p. 18 (2000). [2] P.R. Solanki, et al., NPG Asia Material, vol. 3(1), p. 17 (2011). [3] V.L. Venkatraman, et. al. Biosens. & Bioelectr. vol. 24, p.3078 (2009). [4] Wen-Ding Huang, et. al. Sensors and Actuators: A, vol. 169, p. 1, (2011). [5] M. Pourbaix, Atlas of electrochemical equilibria in aqueous solutions, National Association of Corrosion Engineers p. 374, 1974.

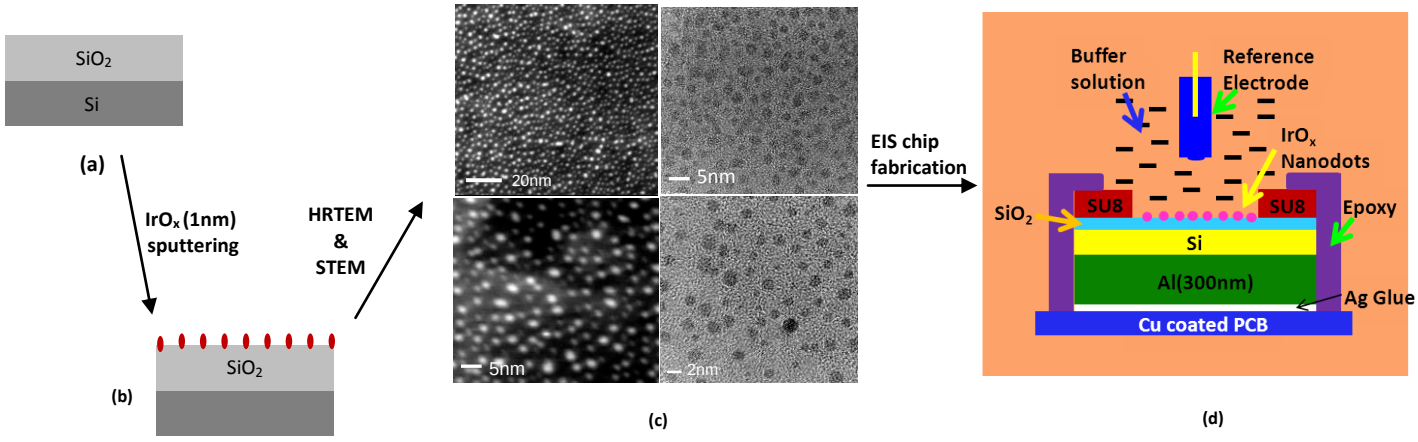

Fig. 1 Schematic view of the fabrication process of iridium oxide (IrO_x) nanodots (NDs) modified EIS sensor chip. (a) 40nm SiO_2 deposition with thermal oxidation, (b) IrO_x NDs deposition using RF sputtering technique, (c) Plane view STEM/HRTEM images to calculate size and density of NDs distribution, and (d) schematic view of EIS sensor chip. A high density of $1.18x10^{13}/cm^2$ is observed for as-deposited IrO_x-NDs.

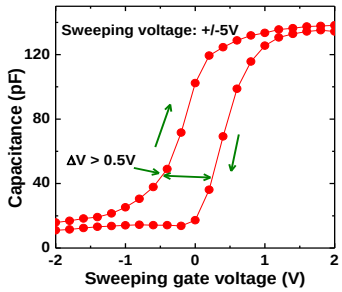

Fig. 2 Charge trapping behavior of IrO_x NDs by fabricating as flash memory device in an $IrO_x/Al_2O_3/IrO_x$-NDs/Al_2O_3/SiO_2 /n-Si structure.

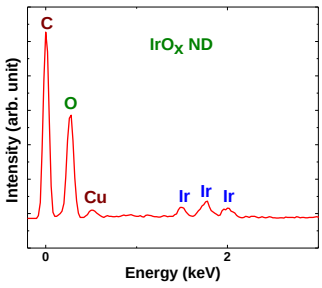

Fig. 3 EDX spectrum of IrO_x NDs deposited on the SiO_2 surface.

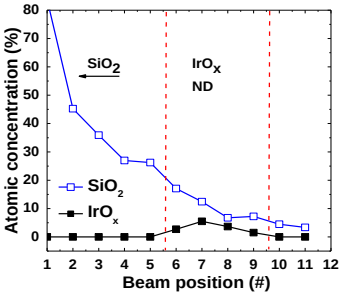

Fig. 4 EDX depth profile of IrO_x nanodots deposited on the SiO_2 surface.

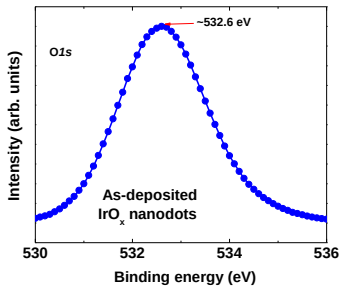

Fig. 5 XPS analysis of O1s signal of as-deposited IrO_x nanodots.

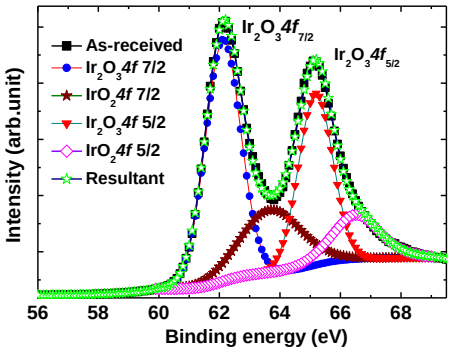

Fig. 6 XPS analysis of as-deposited IrO_x nanodots confirms the formation of respective oxides.

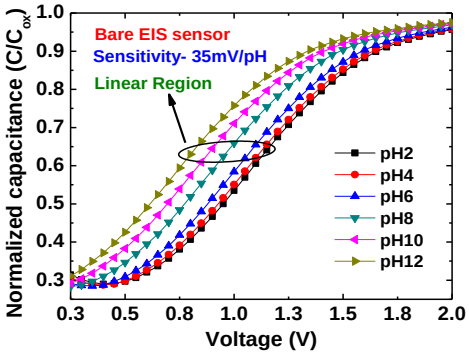

Fig. 7 The C-V curve of bare SiO_2 sensor in different pH buffer solutions.

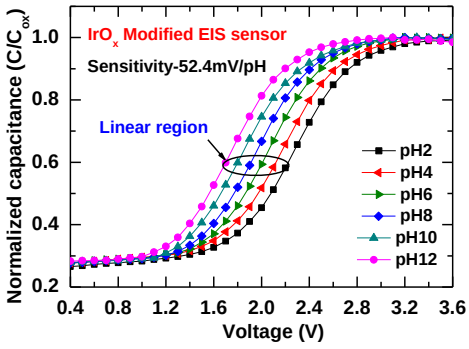

Fig. 8 The CV curve of IrO_x nanodots modified EIS sensor.

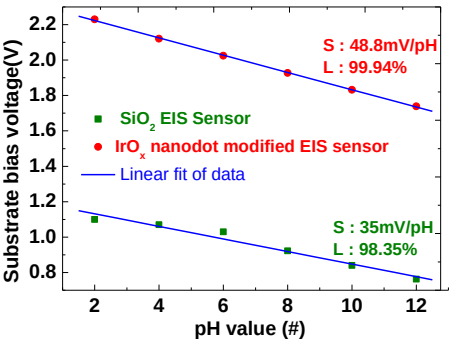

Fig. 9 Comparative sensitivity of bare SiO_2 and IrO_x nanodots modified EIS sensor.

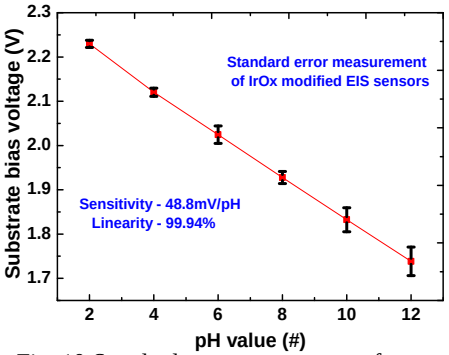

Fig. 10 Standard error measurement from the three successive IrO_x modified EIS sensor.

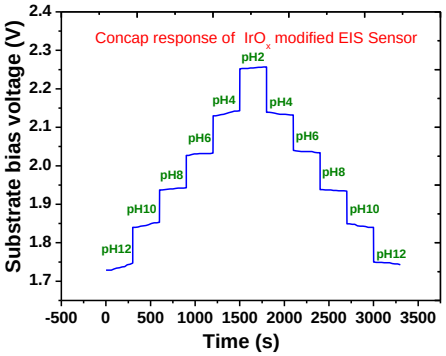

Fig. 11 Concap response of IrO_x modified EIS sensor.